

Dynamical Friction from field particles with a mass spectrum

L. Ciotti

*Dept. of Astronomy, University of Bologna,
via Ranzani 1, 40127 Bologna, Italy*

The analytical generalization of the classical dynamical friction formula (derived under the assumption that all the field particles have the same mass) to the case in which the masses of the field particles are distributed with a mass spectrum is presented. Two extreme cases are considered: in the first, energy equipartition is assumed, in the second all the field particles have the same (Maxwellian) velocity distribution. Three different mass spectra are studied in detail, namely the exponential, discrete (two components), and power-law cases. It is found that the dynamical friction deceleration can be significantly stronger than in the equivalent classical case, with the largest differences (up to a factor of 10 or more in extreme cases) arising for test particle velocities comparable to the mass-averaged velocity dispersion of the field particles. The present results are relevant to our understanding of the dynamical evolution of globular clusters, in particular in the modelization of mass segregation and sedimentation of Blue Straggler stars and Neutron stars, and for the study of binary black holes in galactic nuclei.

INTRODUCTION

Dynamical Friction is a very interesting physical phenomenon, with important applications in Astrophysics (and in Plasma Physics). At the simplest level, it can be described as the slowing-down of a test particle moving in a sea of field particles, due to the cumulative effect of long-range interactions (no geometrical collisions are considered). Several approaches have been devised to understand the underlying physics (which is intriguing, as the final result is an irreversible process produced by a time-reversible dynamics). Here I recall the kinetic approach pioneered among others by Chandrasekhar, Spitzer and von Neumann (e.g., see [1]-[3]; for a more readable mathematical account see also [4]-[7]). More sophisticated approaches, based on a different physical description of the phenomenon (e.g., taking also in account the mutual interactions of the field particles, and more realistic inhomogeneous systems), have been also developed and applied to the case of spherical systems (e.g., see [8] and references therein). A very large body of literature has been dedicated to the study of the astrophysical consequences of dynamical friction in astronomical systems, ranging from the sinking of globular clusters within their host galaxy, to the formation of cD galaxies, to the dynamical evolution of binary black holes in galactic nuclei (e.g., see [9]-[16]). Differences have been found between dynamical friction in Newtonian gravity with Dark Matter and in equivalent MOND systems ([17, 18]); dynamical friction has been also considered when the gravitational drag is produced by a gaseous (instead of discrete) *wake* behind the test object (e.g. [19], and references therein). An extension of the theory to systems anisotropic in the velocity space has been also developed ([20]).

In the classical approach to dynamical friction all the field particles have the same mass, their distribution is uniform in configuration space, and isotropic in the velocity space. Curiously, in the enormous literature on the subject, the case of a *mass spectrum* of the field particles has not attracted much attention. Presumably, the reason behind is the expectation that a very massive test object, several orders of magnitude heavier than the field masses (as often is the case in astrophysical application), should experience the same drag force in a mass spectrum as in the classical case, provided the total mass density of field particles is the same in the two cases.

However, as we will see, *there are* astrophysical situations in which a mass spectrum can have relevant effects, namely when the test particle (even though very massive) travels with a velocity comparable to the velocity dispersion of field particles, or when its mass is of the same order of magnitude of the average mass of the field masses. When the two features are present, the dynamical friction evaluated in the classical case can be underestimated up to a factor of 10 or more, with important consequences for dynamical friction times. A specific example is represented by the population of Blue Straggler stars (BSS) in globular clusters (e.g., see [21]). In fact, BSS are believed to be originated by merging or mass accretion on otherwise normal stars, so that their mass is at most a factor of few larger than the average mass of the stars in the parent cluster, and their mean velocities are similar to those of the normal field stars; in addition, the stars of the globular clusters are characterized by a mass spectrum, and finally, globular clusters are collisional systems, with relaxation and dynamical friction times comparable to their age. Observations also reveal that the radial distribution of BSS in globular clusters can be bimodal. In order to understand the possible origin of such distribution a more accurate description of dynamical friction is needed. Other cases of test particles (with much larger masses) moving with a velocity similar to that of field particles is represented by binary black holes in galactic nuclei. These examples seem to indicate that a study of dynamical friction in a field particle distribution with a mass spectrum is important.

THE CLASSICAL CASE

In order to set the stage for calculations to be performed in the mass spectrum case, we begin with a short review of the most important logical steps used in the derivation of dynamical friction in the classical case. The dynamical friction deceleration on a test mass M moving with velocity \mathbf{v}_t in a homogeneous and isotropic distribution (both in the configuration and in the velocity space) of identical field particles of mass m and number density n , is

$$\frac{d\mathbf{v}_{t||}}{dt} = -4\pi G^2 nm(M+m) \ln \bar{\Lambda} \frac{\Xi(v_t)}{v_t^3} \mathbf{v}_t, \quad v_t \equiv ||\mathbf{v}_t||, \quad (1)$$

where $\ln \bar{\Lambda}$ is the velocity-averaged Coulomb logarithm, the phase-space density distribution of field masses is given by

$$DF = n g(v_f), \quad v_f \equiv ||\mathbf{v}_f||, \quad (2)$$

and g is a positive function dependent on the modulus of the velocity of field particles, \mathbf{v}_f . Finally, the fractional velocity volume function is

$$\Xi(v_t) = 4\pi \int_0^{v_t} g(v_f) v_f^2 dv_f, \quad (3)$$

with the normalization condition $\Xi(\infty) = 1$.

In the traditional approach, eq. (1) can be obtained as follows. The basic idea is to add (vectorially) the orbital deflections of the test particle in n hypothetically independent two-body encounters with each of the field particles. As is well known, the total velocity change along a given unbound orbit in a generic (escaping) force field, obeying the Newton Third Law of Dynamics, is rigorously given by

$$\Delta \mathbf{v}_t = \frac{\mu}{M} \Delta \mathbf{V}, \quad \mu = \frac{mM}{M+m}, \quad (4)$$

where $\mathbf{V} = \mathbf{v}_t - \mathbf{v}_f$ is the pair relative velocity. In each encounter under the action of the r^{-2} force, the vectorial change $\Delta \mathbf{V}$ of the relative velocity is obtained by using the solution of the hyperbolic two-body problem.

Here, however, we obtain the change $\Delta \mathbf{V}_{||}$ in the direction parallel to the initial relative velocity by using the impulsive approximation combined with energy conservation along the relative orbit. For each pair it can be proved that the change of the relative velocity *perpendicular* to the initial relative velocity \mathbf{V} (of modulus $V = ||\mathbf{V}||$) is

$$\mu ||\Delta \mathbf{V}_{\perp}|| \sim \frac{2GMm}{bV}. \quad (5)$$

The formula above is asymptotically exact in the limit of large impact parameter b or large initial relative velocity V . In this case energy conservation along each relative orbit, $V^2 = ||\mathbf{V} + \Delta \mathbf{V}_{||} + \Delta \mathbf{V}_{\perp}||^2$, shows that to the first order (consistent with the adopted impulsive approximation)

$$\Delta \mathbf{v}_{t||} = \frac{\mu \Delta \mathbf{V}_{||}}{M} \sim -\frac{\mu}{M} \frac{||\Delta \mathbf{V}_{\perp}||^2}{2V^2} \mathbf{V} = -\frac{2G^2 m(M+m)}{b^2 V^4} \mathbf{V}. \quad (6)$$

Note that the dependence of $||\Delta \mathbf{v}_{t||}||$ as the inverse of the cube of the initial relative velocity is asymptotically correct only in the impulsive approximation: for slow or grazing orbits the functional dependence of $||\Delta \mathbf{v}_{t||}||$ on V is different. However, as in gravitational plasmas there is no screening effect, it can be proved that the main contribution to dynamical friction comes mainly from distant interactions (e.g. [3]) so that the above term is the leading term. In any case, it is worth to recall that a calculation with the full solution of the two-body problem is straightforward.

We have now to sum over all the encounters. Simple geometry shows that their number in the time interval Δt , impact parameter between b and $b + db$, and with field particles in the differential velocity volume $d^3 \mathbf{v}_f$ is

$$\Delta n_{\text{enc}} = 2\pi b db ||\mathbf{v}_t - \mathbf{v}_f|| \Delta t n g(v_f) d^3 \mathbf{v}_f. \quad (7)$$

Therefore, the differential change of the test particle velocity parallel to the initial relative velocity is

$$\frac{\Delta \mathbf{v}_{t||}}{\Delta t} = -\frac{4\pi G^2 nm(M+m)g(v_f)\mathbf{V}}{bV^3} db d^3 \mathbf{v}_f. \quad (8)$$

Integration over the impact parameter is a delicate step. In fact, in the impulsive approximation an artificial divergence appears for $b = 0$. From the full solution of the two body problem it is easy to show that such divergence disappears (but the divergence for $b \rightarrow \infty$ cannot be eliminated in an infinite system). The final result after integration over the impact parameter can be expressed by introducing the *Coulomb logarithm* $\ln \Lambda$, where the quantity Λ depends¹ on M, m, V . Equation (8) becomes

$$\frac{d\mathbf{v}_{t||}}{dt} = -4\pi G^2 nm(M+m) \ln \Lambda \frac{g(v_f)(\mathbf{v}_t - \mathbf{v}_f)}{||\mathbf{v}_t - \mathbf{v}_f||^3} d^3 \mathbf{v}_f. \quad (9)$$

We now integrate over the velocity space. Following Chandrasekhar ([2]), we introduce the *velocity weighted Coulomb logarithm* $\ln \bar{\Lambda}$, and therefore the Newton theorem on spherical shells (here applied to velocity space given the assumed isotropy of the velocity distribution of field particles), leads to the identity

$$\int \ln \Lambda \frac{g(v_f)(\mathbf{v}_t - \mathbf{v}_f)}{||\mathbf{v}_t - \mathbf{v}_f||^3} d^3 \mathbf{v}_f = \ln \bar{\Lambda} \frac{\Xi(v_t)}{v_t^3} \mathbf{v}_t, \quad (10)$$

which proves eq. (1). The cumulative effect of the encounters is to slow-down the test particle in the direction of the test particle velocity itself. This is not trivial, as according to eq. (6) the deceleration in each single encounter is parallel to the *relative* velocity, and not to \mathbf{v}_t . However, when summing over all the encounters, the average value of the field velocity component vanishes by assumption of isotropy.

We conclude this preparatory Section by recalling that in the commonly considered case of a Maxwellian velocity distribution for the field particles, the function g in eq. (2) and the velocity volume function in eq. (3) are

$$g(v_f) = \frac{e^{-v_f^2/(2\sigma_0^2)}}{(2\pi)^{3/2}\sigma_0^3}, \quad \Xi(v_t) = \text{Erf}(\tilde{v}_t) - \frac{2\tilde{v}_t e^{-\tilde{v}_t^2}}{\sqrt{\pi}}, \quad (11)$$

where $\tilde{v}_t \equiv v_t/(\sqrt{2}\sigma_0)$ is the normalized test particle velocity, and

$$\text{Erf}(x) = \frac{2}{\sqrt{\pi}} \int_0^x e^{-t^2} dt \quad (12)$$

is the standard Error Function. A final comment, of central importance in the following discussion, is in order here. According to eqs. (1) and (3) only field particles *slower*

¹ Actually, the exact integration over the impact parameter based on hyperbolic orbits leads to the expression $0.5 \ln(1 + \Lambda^2) \simeq \ln \Lambda$, where $\Lambda = b_{\max}/[G(M+m)]$ and b_{\max} is a fiducial maximum impact parameter (e.g., see [7]).

than the test particle contribute to its deceleration. This sharp “cut” in velocity space results from the different assumptions, namely 1) that the velocity distribution of field particles is isotropic, 2) that we can take the Coulomb logarithm outside the integral in eq. (10), and finally 3) that the velocity change in each encounter is exactly proportional to V^{-2} (as in the first order impulsive approximation adopted here). A more general analysis can be done, in which the (small) correcting terms can be explicitly evaluated (e.g., see [22]). In any case, in the presence of a mass spectrum of field particles at equipartition, the resulting “drag” force is determined by the combined effect of the mass function (in astrophysical applications usually peaked at low masses) *and* the fact that the more massive particles, responsible for large decelerations, move slower; therefore, in principle there is an interesting compensating effect between number density, mass of field particles relative to the test particle, and number density in velocity space.

MASS SPECTRUM: THE GENERAL CASE

With the previous preparatory work, it is now easy to generalize the classical dynamical friction formula (1) to the case of a mass spectrum of field particles. A generic mass spectrum with isotropic velocity distribution is described in phase-space, by extension of the classical treatment, with a function

$$DF = \Psi(m) g(v_f, m), \quad (13)$$

where the associated total number density of field particles and the average mass of the spectrum $\Psi(m)$ are

$$n = \int_0^\infty \Psi(m) dm, \quad n \langle m \rangle = \int_0^\infty m \Psi(m) dm, \quad (14)$$

so that the normalization of the velocity distribution for each mass component leads to the condition

$$\Xi(v_t, m) = 4\pi \int_0^{v_t} g(v_f, m) v_f^2 dv_f, \quad \Xi(\infty, m) = 1 \quad \forall m. \quad (15)$$

In order to compare the dynamical friction in presence of a mass spectrum with the classical case, we must carefully define the concept of the *equivalent* classical system. We will say that a classical system is equivalent to a mass spectrum case if 1) the number density in the classical case is the same as the *total* number density in the mass spectrum case; 2) the field mass m in the classical case is the same as the *average* field mass $\langle m \rangle$; 3) the velocity dispersion of the Maxwellian velocity distribution in the classical case is the same as the *equipartition* velocity dispersion of the mass spectrum case. We can summarize the above conditions by saying that the comparison is between two systems with the same number, mass, and kinetic energy density of the field particles. Similar comments, but different answers, apply when instead of equipartition among the different species, all the field particles with a mass spectrum share the same velocity distributions (for example as expected in a collisionless system made of stars and dark matter).

In the equipartition case, we use as 1-dimensional equipartition velocity dispersion the one relative to the average mass, i.e., we assume

$$m\sigma_m^2 = \langle m \rangle \sigma_0^2, \quad g(v_f, m) = \frac{e^{-v_f^2/(2\sigma_m^2)}}{(2\pi)^{3/2}\sigma_m^3} = \frac{e^{-rv_f^2/(2\sigma_0^2)}r^{3/2}}{(2\pi)^{3/2}\sigma_0^3}, \quad r \equiv \frac{m}{\langle m \rangle}, \quad (16)$$

so that from eq. (15)

$$\Xi(v_t, m) = \text{Erf}(\tilde{v}_t\sqrt{r}) - \frac{2\tilde{v}_t\sqrt{r}e^{-\tilde{v}_t^2 r}}{\sqrt{\pi}}, \quad (17)$$

where again $\tilde{v}_t = v_t/(\sqrt{2}\sigma_0)$. In the present case the differential number of encounters suffered by the test particle is

$$\Delta n_{\text{enc}} = 2\pi b db \|\mathbf{v}_t - \mathbf{v}_f\| \Delta t \Psi(m) g(v_f, m) dm d^3\mathbf{v}_f. \quad (18)$$

Therefore, by summing the formula obtained in the classical treatment over all the species, the deceleration in the mass spectrum case is given by

$$\begin{aligned} \frac{d\mathbf{v}_{t\parallel}}{dt} &= -4\pi G^2 \langle \ln \bar{\Lambda} \rangle \frac{\mathbf{v}_t}{v_t^3} \int_0^\infty \Psi(m) m(M+m) \Xi(v_t, m) dm \\ &= -4\pi G^2 n \langle m \rangle (M + \langle m \rangle) \langle \ln \bar{\Lambda} \rangle \frac{\Xi^*(v_t)}{v_t^3} \mathbf{v}_t, \end{aligned} \quad (19)$$

where now $\langle \ln \bar{\Lambda} \rangle$ is the mass-averaged Coulomb logarithm. The second of the above equations is just the definition of the new velocity coefficient Ξ^* . In practice, from the knowledge of this last function one can derive the dynamical friction deceleration in case of a mass spectrum by using the same formalism of the classical case, where m is replaced by $\langle m \rangle$. In all the following computations we will assume that $\langle \ln \bar{\Lambda} \rangle \simeq \ln \bar{\Lambda}$.

It is important to note that, for *large* velocities of the test particle the velocity volume factor $\Xi(v_t, m)$ tends to unity, and therefore, *the values of the dynamical friction deceleration in the high-velocity limit can be also interpreted as the scaling factor between the classical and mass spectrum case when all the species in the mass spectrum have the same velocity dispersion*. This case is of astrophysical importance, for instance for dark matter halos in galaxies, where dark matter particles and stars likely are *not* at the equipartition. We now study a few explicit cases of mass spectrum amenable to analytic solutions, so that the differences with the equivalent classical cases can be quantified.

EXPONENTIAL SPECTRUM

In this case the mass spectrum is given by

$$\Psi(m) = \frac{ne^{-m/\langle m \rangle}}{\langle m \rangle}. \quad (20)$$

The integral over masses in eq. (19) can be performed analytically by inverting the order of integration between m and v_f . The result is

$$\int_0^\infty \Psi(m) m (M + m) \Xi(v_t, m) dm = n \langle m \rangle^2 [\mathcal{R} H_1(\tilde{v}_t) + H_2(\tilde{v}_t)], \quad \mathcal{R} \equiv \frac{M}{\langle m \rangle}. \quad (21)$$

In practice, the mass ratio \mathcal{R} measures the mass of the test particle in units of the average mass of the field particles. From eqs. (19) and (21) it follows that the associated velocity factor can be written as

$$\Xi^*(v_t) = \frac{\mathcal{R} H_1(\tilde{v}_t) + H_2(\tilde{v}_t)}{\mathcal{R} + 1}, \quad (22)$$

with the surprisingly simple result

$$H_1(\tilde{v}_t) = \frac{\tilde{v}_t^3 (5 + 2\tilde{v}_t^2)}{2(1 + \tilde{v}_t^2)^{5/2}}, \quad H_2(\tilde{v}_t) = \frac{\tilde{v}_t^3 (35 + 28\tilde{v}_t^2 + 8\tilde{v}_t^4)}{4(1 + \tilde{v}_t^2)^{7/2}}. \quad (23)$$

As expected, eqs. (22) and (23) prove that the result coincides asymptotically with the classical case for fast ($H_1 \sim 1$ and $H_2 \sim 2$) and massive ($\mathcal{R} \gg 1$) test particles. In general, as can be seen from Fig. 1, the velocity factor in the case of exponential mass spectrum with equipartition is larger than in the corresponding classical case (heavy line): for massive test particles the maximum drag (corresponding to $v_t \simeq 0.81\sigma_0$) is a factor ≈ 2 higher than in the equivalent classical case. The dynamical friction time is correspondingly shorter, with significant discrepancies for test particles moving with velocities comparable to the equipartition velocity dispersion of the field particles. Finally, the leading term of eq. (22) for $v_t \rightarrow \infty$ shows that in the non equipartition case the correcting factor to be adopted when using the classical formula is $(2 + \mathcal{R})/(1 + \mathcal{R})$, so that for \mathcal{R} of order of unity the classical formula underestimates the dynamical friction deceleration by a factor ≈ 1.5 .

DISCRETE SPECTRUM

For the case of a system made of two species of field particles the mass spectrum is

$$\Psi(m) = n_1 \delta(m - m_1) + n_2 \delta(m - m_2). \quad (24)$$

With the convenient introduction of the dimensionless parameters $x \equiv n_2/n_1$ and $y \equiv m_2/m_1$, it follows that

$$n = (1 + x)n_1, \quad \langle m \rangle = \frac{n_1 m_1 + n_2 m_2}{n_1 + n_2} = \frac{1 + xy}{1 + x} m_1; \quad (25)$$

the limit $y = 1$ recovers the classical case. The generalization to an arbitrary number of different field components presents no difficulties. The mass integration in eq. (19) is immediate, the result is formally identical to eqs. (21) and (22), while from eqs. (24) and (17) we now have

$$H_1 = \frac{\Xi(v_t, m_1) + xy \Xi(v_t, m_2)}{1 + xy}, \quad H_2 = \frac{(1 + x)[\Xi(v_t, m_1) + xy^2 \Xi(v_t, m_2)]}{(1 + xy)^2}. \quad (26)$$

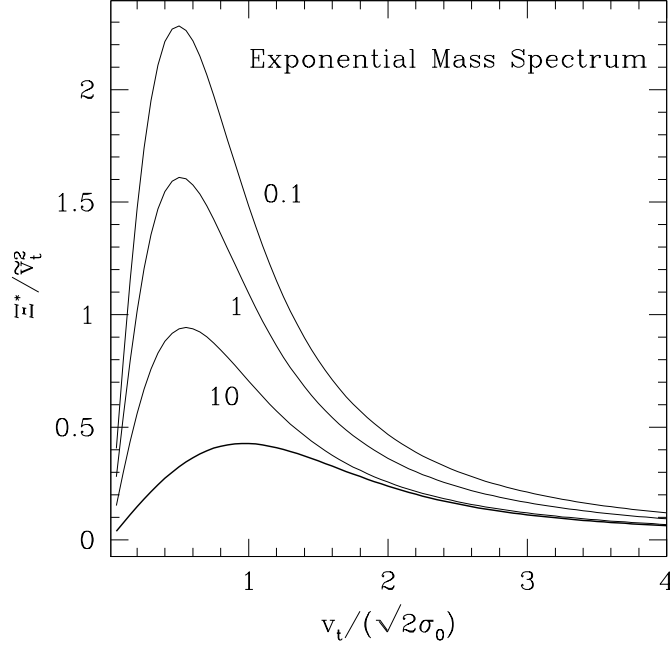


FIGURE 1. The velocity coefficient Ξ^*/\tilde{v}_t^2 in eq. (19) for the Exponential Mass Spectrum case with equipartition; $\tilde{v}_t = v_t/(\sqrt{2}\sigma_0)$. The curves (from top to bottom) correspond to a test particle with mass 0.1, 1, and 10 times the average mass of the spectrum, respectively. Mass ratios larger than ~ 10 produce curves almost identical to the $\mathcal{R} = 10$ case. The heavy solid line represents the velocity coefficient of the equivalent classical case, i.e. when the field masses are all identical, and their number density, average mass, and kinetic energy density are the same as in the mass spectrum case.

For low velocities of the test particle one finds the asymptotic trends

$$H_1 \sim \frac{4v_t^3(1+x)^{3/2}(1+xy^{5/2})}{3\sqrt{\pi}(1+xy)^{5/2}}, \quad H_2 \sim \frac{4v_t^3(1+x)^{5/2}(1+xy^{7/2})}{3\sqrt{\pi}(1+xy)^{7/2}}. \quad (27)$$

In turn, for large velocities of the test particle the leading terms are

$$H_1 \sim 1, \quad H_2 \sim \frac{(1+x)(1+xy^2)}{(1+xy)^2}. \quad (28)$$

Therefore, for fast and massive test particles, the dynamical friction force in the presence of equipartition is the same as in the equivalent classical case. In the non equipartition case, the correcting factor for the classical dynamical friction formula is obtained by evaluating eq. (22) with the expansions given in eq. (28).

We now study the case of arbitrary mass ratios and velocities. For simplicity we restrict the following analysis to the special case of a system in which the densities of the

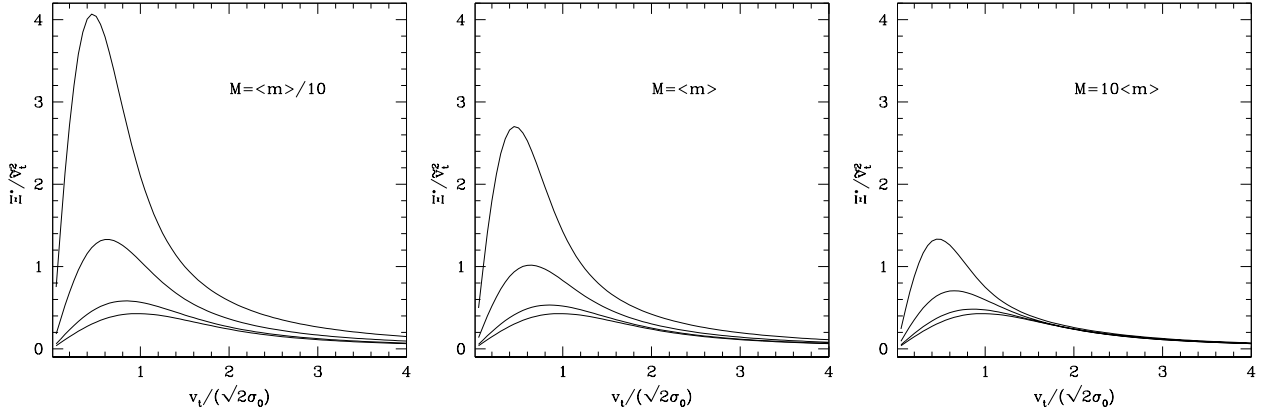


FIGURE 2. The velocity coefficient Ξ^*/\tilde{v}_t^2 in eq. (19) for the Discrete Mass Spectrum case with two species in equipartition and with the same mass density, i.e. $n_1 m_1 = n_2 m_2$. The panels (from left to right) correspond to mass ratios $\mathcal{R} = 0.1, 1, 10$, while the curves in each panel (in decreasing order) correspond to number ratios $n_2/n_1 = x = 8, 4, 2$, respectively. For increasing mass ratio \mathcal{R} and large velocities of the test particle the deceleration tends to the value obtained in the equivalent classical case.

species 1 and 2 are the same, i.e., $n_1 m_1 = n_2 m_2$. From the definitions in eq. (25) it follows that $xy = 1$. Therefore, for $x > 1$ the masses m_2 are lighter and more numerous than the species 1; it is easy to recognize that the cases $x > 1$ and $x < 1$ (with reciprocal values) are coincide. In Fig. 2 the situation is illustrated for three different mass ratios \mathcal{R} and different number ratios of the two field species. The qualitative trend is the same as in the exponential case: the equivalent classical case always underestimates the true value of dynamical friction, with largest deviations (at fixed \mathcal{R}) for test particle velocities comparable to the field equipartition velocity dispersion. The discrepancies can be as large as a factor 6 - 10 for masses of the test particle of the same order of magnitude of the average mass of the spectrum. Similar calculations can be done on the other relevant case of identical *number* density of the two species, $n_1 = n_2$ (i.e., $x = 1$), and again the results for the mass spectrum case shows that the frictional force is stronger than in the equivalent classical case.

POWER-LAW SPECTRUM

As commonly done in many cases of astrophysical interest, we finally assume a power-law spectrum peaked at low masses, with a minimum mass m_i , a finite average mass $\langle m \rangle$, and exponent $a > 1$, i.e.

$$\Psi(m) = \frac{nam_i}{m^{1+a}}, \quad \langle m \rangle = \frac{am_i}{a-1}, \quad m \geq m_i. \quad (29)$$

As in the two previous cases, mass integration in eq. (19) can be done analytically. Equations (21) and (22) remain unchanged, while now

$$H_1(\tilde{v}_t) = \text{Erf}(\tilde{v}_t \sqrt{c}) - \frac{(2a-3)\sqrt{c}\tilde{v}_t E_{a-1/2}(c\tilde{v}_t^2)}{\sqrt{\pi}}, \quad (30)$$

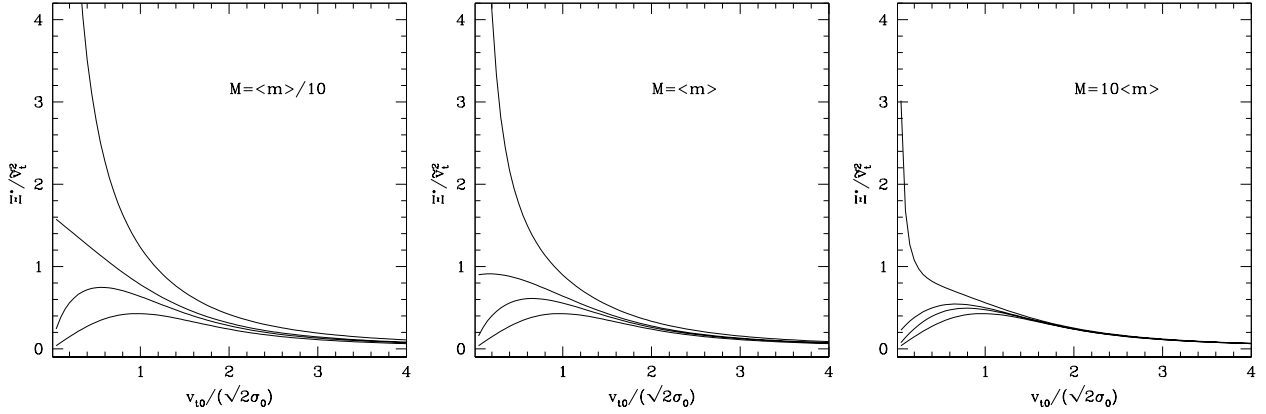


FIGURE 3. The velocity coefficient Ξ^*/\tilde{v}_t^2 in eq. (19) for the Power-Law Mass Spectrum case in equipartition. The panels (from left to right) correspond to mass ratios $\mathcal{R} = 0.1, 1, 10$, while the curves in each panel (in decreasing order) correspond to exponent $a = 2.5, 3, 3.5$, respectively. As in the previous cases, for increasing mass ratio \mathcal{R} and large velocities of the test particle the deceleration converges to the value obtained in the corresponding classical case.

$$H_2(\tilde{v}_t) = \frac{(a-1)^2}{a(a-2)} \left[\text{Erf}(\tilde{v}_t\sqrt{c}) - \frac{(2a-5)\sqrt{c}\tilde{v}_t E_{a-3/2}(c\tilde{v}_t^2)}{\sqrt{\pi}} \right]. \quad (31)$$

The convergence of the H_2 function in integral (21) requires $a > 2$. This condition may be relaxed if a cut-off on large masses is applied to the mass spectrum. The transcendent function appearing in the two expressions above is the Exponential Integral, which is related to the left incomplete Euler Gamma Function as

$$E_k(z) \equiv \int_1^\infty t^{-k} e^{-tz} dt = z^{k-1} \Gamma(1-k, z). \quad (32)$$

It is easy to show that, for large velocity of the test mass, asymptotically

$$H_1 \sim 1, \quad H_2 \sim \frac{(a-1)^2}{a(a-2)}. \quad (33)$$

Therefore, this demonstrates again that for high velocity and large mass of the test particle the classical result is recovered. The expansion for vanishingly small v_t requires that different cases must be distinguished. In general, when $a > 7/2$ both the H_1 and H_2 functions both vanish as \tilde{v}_t^3 , while $H_1 = \mathcal{O}(\tilde{v}_t^{2a-2})$ for $a < 5/2$ and $H_2 = \mathcal{O}(\tilde{v}_t^{2a-4})$ for $a < 7/2$. In the critical cases the functions H_1 and H_2 vanish as $\mathcal{O}(-\tilde{v}_t^3 \ln \tilde{v}_t)$. Note that the function Ξ^*/\tilde{v}_t^2 diverges for $\tilde{v}_t \rightarrow 0$ when $a < 3$ as a consequence of the H_2 behavior, while it reaches a finite value when $a = 3$. In Fig. 3 some representative case is illustrated, for different values of \mathcal{R} and of the power-law index a . The corrective factor for the classical formula when the field particles are not at the equipartition, but are characterized by the same Maxwell distribution independently of their mass, is obtained by inserting the functions in eq. (33) in eq. (22).

CONCLUSIONS

In this paper I presented a generalization of the standard dynamical friction formula to the case of a test particle moving in a homogeneous distribution of field particles characterized by a mass spectrum. Surprisingly, the mass spectrum problem has not received much attention in the astrophysical literature. In the present investigation the velocity distribution of each species of the field particles is Maxwellian, and equipartition among the species is assumed. It has been also shown how the situation in which all the field particles have the same velocity distribution can be easily recovered as a limit case of the equipartition analysis.

The comparison with the classical case is done by considering an equivalent classical system in which 1) the field particles have the same mass as the average mass of the mass spectrum case, 2) the number density is equal to the total number density in the mass spectrum case, and finally 3) the velocity dispersion of the classical case equals the equipartition velocity dispersion in the mass spectrum case. In practice, the classical and the mass spectrum cases have the same number density, mass density, and kinetic energy content of the field masses. Three specific cases of mass spectrum (i.e., an exponential mass spectrum, a two-component discrete spectrum, and a power-law spectrum) have been considered, and the associated analytical formulae derived.

A few common trends are noted. First, for *fast* and *massive* test particles the results in the classical and in mass spectrum cases are asymptotically identical, because for high velocities the velocity volume factor tends to unity, and for large test masses the specific form of the mass spectrum becomes irrelevant, as all the field particles can be considered vanishingly small, and only the mass density of field particles appears in the relevant expressions of the friction coefficient.

Second, in *all* the cases considered, the dynamical friction force in the mass spectrum case is larger than in the corresponding classical case. The largest differences are found for test particle masses comparable to the average mass of the spectrum, and test particle velocities close to the equipartition velocity dispersion. The differences can be as high as a factor of 10 or more. The dynamical friction times are correspondingly reduced.

Third, for very large velocities of the test particle, but for a test mass particle comparable to the average mass of the spectrum (say $\mathcal{R} < 10$), there are differences between the mass spectrum case and the classical case. From the astrophysical point of view this last result also applies to the case in which the mass spectrum particles are *not* at the equipartition, but the species are characterized by the same velocity dispersion (for example, stars and dark matter particles in the common potential well).

It follows that the classical dynamical friction formula for a very massive object (such as a globular cluster or a mini dark matter halo) sinking into a larger system, made of stars and dark matter, should provide correct values for the dynamical friction force (as far as the sinking velocity is large). However, there are astronomical systems where the present investigation is relevant, i.e., the case of Blue Straggler stars in globular clusters. In fact, 1) BSS stars have a mass slightly larger than the average mass of the field stars in the host system; 2) the velocity of BSS is close to the local velocity dispersion of the field stars, just because they are orbiting in the parent globular cluster; 3) the field stars in a globular cluster are characterized by a mass spectrum, and the assumption of equipartition is reasonable, because of the quasi-relaxed state of globular

clusters. If the three points above apply, then it follows that the adoption of the classical dynamical friction formula to study the evolution of the spatial distribution of BSS (or neutron stars) in globular clusters may be inaccurate, with prediction of excessive sinking times. It would be very interesting to study whether the formulae derived in this paper succeeds in explaining the observed radially bimodal distribution of BSS in some well studied globular cluster; an important issue here is how the initial mass function of the field stars is modified at each radius by dynamical evaporation of low mass stars, with the obvious consequence of a reduction of the spanned mass interval. Another case of possible interest is represented by the initial stages of the dynamical evolution of binary black holes in galactic nuclei. Finally, from a theoretical point of view, it would also be interesting to extend the present treatment to the evaluation of the two-body relaxation time in the presence of a mass spectrum.

ACKNOWLEDGMENTS

I wish to thank G. Bertin, J. Binney, F. Pegoraro and M. Stiavelli for very useful comments.

REFERENCES

1. S. Chandrasekhar, and J. von Neumann, *ApJ*, **97**, 1–27 (1943).
2. S. Chandrasekhar *Principles of Stellar Dynamics*, Dover, New York, USA, 1960 (originally published in 1943)
3. L. Spitzer *Dynamical Evolution of Globular Clusters*, Princeton University Press, Princeton, USA, 1987
4. K. F. Ogorodnikov *Dynamics of Stellar Systems*, Pergamon, Oxford, UK, 1965
5. G. Bertin, *Dynamics of Galaxies*, Cambridge University Press, Cambridge, UK, 2000
6. L. Ciotti *Lecture Notes on Stellar Dynamics*, Scuola Normale Superiore, Pisa, Italy, 2000
7. J. Binney, and S. Tremaine, *Galactic Dynamics*, Princeton University Press, Princeton, USA, 2008 (2nd Ed.)
8. S. Tremaine, and M. D. Weinberg, *MNRAS*, **209**, 729–757 (1984).
9. S. Tremaine, J. P. Ostriker, and L. Spitzer *ApJ*, **196**, 407–411 (1975).
10. S. D. M. White *MNRAS*, **174**, 19–28 (1976).
11. J. P. Ostriker, and M. A. Hausman *ApJ*, **217**, L125–L129 (1977).
12. T. R. Bontekoe, and T. S. van Albada *MNRAS*, **224**, 349–366 (1987).
13. G. Bertin, T. Liseikina, and F. Pegoraro *A&A*, **405**, 73–88 (2003).
14. C. Nipoti, T. Treu, L. Ciotti, and M. Stiavelli *MNRAS*, **355**, 1119–1124 (2004).
15. D. Merritt *Reports on Progress in Physics*, **69**, 2513–2579 (2006).
16. S. E. Arena, and G. Bertin *A&A*, **463**, 921–935 (2007).
17. L. Ciotti, and J. Binney *MNRAS*, **351**, 285–291 (2004).
18. C. Nipoti, L. Ciotti, J. Binney, and P. Londrillo *MNRAS*, **386**, 2194–2198 (2008).
19. N. Fathi *MNRAS*, **401**, 319–332 (2010).
20. J. Binney *MNRAS*, **181**, 735–746 (1977).
21. F. R. Ferraro et al. *Nature*, **462**, 1028–1031 (2009).
22. M. L. White *ApJ*, **109**, 159–163 (1949).